Journal of
Water & Climate Change

IWA PUBLISHING

Journal of Water and Climate Change Vol 16 No 8, 2503 doi: 10.2166/wcc.2025.033

Increasing culvert hydraulic capacity for improved climate resilience: a physical modelling analysis

Thea Maria Dorothea Giliomee *, Ione Loots and Marco van Dijk

Department of Civil Engineering, University of Pretoria, Lynnwood Road, Hatfield, Pretoria, South Africa
*Corresponding author. E-mail: u20424028@tuks.co.za

TMDG, 0009-0004-1582-6865; IL, 0000-0003-0715-6852; MvD, 0000-0002-3830-526X

ABSTRACT

Culverts often fail to handle increased flood peaks due to urbanisation and climate change. Modifying culvert inlets to increase discharge capacity can negate the need for additional culvert barrels or to rebuild the entire structure. Although some previous studies investigated hydraulic culvert improvements, this study is the first to test different combinations of headwall and wingwall angles, and the effect of aeration vents, to improve capacity of inlet-controlled culverts. This physical modelling study evaluates various modified box and circular culvert inlets, quantifies their impact on capacity, develops a coefficient for use in standard equations, and verifies the alignment of results with established references and guidelines. A 15° headwall with a 30° wingwall added to a box culvert or a rounded inlet edge for a circular culvert improved the flow by up to 34% at a headwater depth of twice the culvert height (2*D*), or up to 18% at 1.2*D* for box culverts and 24% at 1.2*D* for circular culverts. An air vent after the inlet had an insignificant influence on the capacity. A novel flow improvement coefficient was developed to calculate improved capacity with existing design equations. Culvert inlet improvements will reduce flood risks and contribute to sustainable drainage infrastructure.

Key words: climate adaptation, climate change, culvert inlet, headwall, urbanisation, wingwall

HIGHLIGHTS

- Modified inlets can be used to adapt culverts to climate change or increased runoff due to urbanisation.
- A combination of different wingwall and headwall angles improves box culvert performance.
- Rounded edge inlets perform better than wingwalls and headwalls for circular culverts.
- Novel flow improvement coefficients can be used to quantify and determine increased culvert capacities.

INTRODUCTION

Extreme and prolonged weather events caused by climate change are placing growing stress on ageing grey infrastructure. This can be addressed by restoring natural riverine landscapes, such as floodplains, and source water wetlands (Skidmore & Wheaton 2022). Large-scale adoption of nature-based solutions and other types of green infrastructure that allow water infiltration or facilitate rain harvesting and decrease flow peaks is another option (Pamungkas & Purwitaningsih 2019; Lallemant *et al.* 2021; Abreu *et al.* 2022). Adaptation infrastructure includes infiltration trenches, dry wells, porous pavement, rain barrels, blue roofs, green roofs, and bioretention (Kirshen *et al.* 2014). While these interventions contribute to climate adaptation and relieve stress on ageing grey infrastructure, Pamungkas & Purwitaningsih (2019) concluded that a combination of green and grey infrastructures can significantly reduce flooding in a water-sensitive and feasible manner. Grey infrastructure is well-established in drainage systems, but it can be modified to become more resilient to climate change.

Culverts play an important role in the stormwater drainage system and transport infrastructure of a country (Jaeger *et al.* 2019). They are designed to convey a specific flow capacity beneath roads, highways or through embankments (Schall *et al.* 2012). Culverts can, however, become insufficient over time due to increasing flood peaks (Cullis *et al.* 2015). Flood peaks for rarer flood events have already increased across many parts of the world due to climate change (Wasko *et al.* 2021). Additionally, continuing urbanisation increases the volume of runoff by increasing impermeable surfaces (Schütte & Schulze 2017).

Therefore, during flood events, inadequate culvert drainage can lead to infrastructure damage, inconvenience for road users, and potential loss of life.

Culverts often discharge a smaller capacity than expected (Straub *et al.* 1953). When the river channel is wider than the culvert barrel, the momentum of water entering a square edge inlet culvert creates a flow contraction, or vena contracta, just after the inlet (Schall *et al.* 2012). At the vena contracta, the cross-sectional flow area is at a minimum, which reduces the culvert capacity (Jaeger *et al.* 2019). Therefore, modifying the culvert inlet to provide a more gradual flow transition at the inlet can increase discharge capacity, as shown and described in Table 1, with a rounded edge inlet as an example of a modified inlet. An optimised culvert design would either increase the culvert capacity for a specific headwater depth or pass the design discharge at the lowest headwater depth (Harrison *et al.* 1972). Therefore, inlet modifications can be used to eliminate the need for rebuilding inadequate culverts, providing a cost-effective solution with minimal disruption to traffic (Jaeger *et al.* 2019).

Under inlet control conditions, inlet improvements can significantly increase the flow through a culvert (Jones *et al.* 2006; Schall *et al.* 2012). However, both inlet and outlet flow controls can benefit from optimised inlet designs (Schall *et al.* 2012; Jaeger *et al.* 2019). Previous studies have tested various inlet modifications. Some of the most promising inlet configurations are:

- Tapered (Schall *et al.* 2012), especially slope-tapered inlets (Harrison *et al.* 1972).
- 15° headwalls (Ashour *et al.* 2016; Aly 2017).
- 45° wingwalls (Yarnell *et al.* 1926; West 1956) followed by 30° wingwalls (West 1956).
- Rounded inlets, rounded at least to 0.15B (culvert width) (Jaeger 2019), rounded to 0.15D (culvert height) (Straub *et al.* 1953; French 1955) or preferably rounded to 0.25D (French 1961; Sellevold *et al.* 2023).
- Bevels angled at 10° (French 1961; Sellevold *et al.* 2023).
- Socket ends (Harrison *et al.* 1972; Schall *et al.* 2012; Buck & Allitt 2019).

In addition to inlet modifications, the installation of an air vent at the inlet region might also improve the culvert discharge capacity since it can ventilate the sub-atmospheric pressures (French 1964). The vented barrel has a smaller wetted perimeter with a similar cross-sectional area, resulting in an increase in velocity (Chadwick *et al.* 2021). However, the effect of aeration vents has not previously been thoroughly tested, and their impact on culvert performance remains unclear.

Discharge equations are typically used to determine culvert dimensions for design flow rates. FHWA Hydraulic Design Series No. 5 (HDS-5) (Schall *et al.* 2012) is the most widely recognised manual on culvert hydraulics (Jaeger *et al.* 2019).

Table 1 | Flow contraction around a square edge inlet and a rounded edge inlet adapted from Yarnell *et al.* (1926), West (1956), Schall *et al.* (2012) and Jaeger (2019)

Square edge inlet	Rounded edge inlet
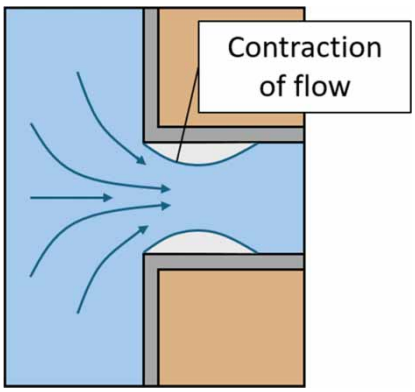	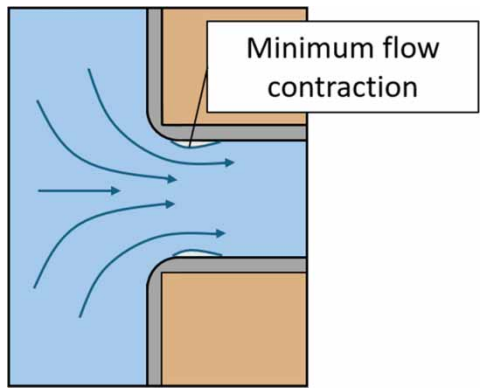
• Flow contraction after the culvert inlet. A smaller cross-sectional area is utilised. Flow becomes highly turbulent. • High velocities are concentrated in the centre. • Less contact friction with a high initial kinetic energy. • Pressure drops near the vena contracta.	• Flow contraction after the inlet is less, and most of the barrel cross-sectional area is utilised. • The smaller the contraction, the better the culvert performance. • More uniform distribution of velocities. • Gradual flow transition that will reduce energy losses.

The majority of past studies on culvert inlet improvements use the HDS-5 equation structure (Jones *et al.* 2006; Buck & Allitt 2019; Jaeger *et al.* 2019). These studies focus on different inlets, including wingwalls, tapered inlets and inlet edges. However, they do not consider a combination of different wingwall and headwall angles typically using the same angle when combined (de Jager & van Dijk 2024) or testing wingwalls and headwalls separately, such as Ashour *et al.* (2016) that determined Cd-coefficients for angled headwalls exclusively.

Therefore, this study aimed to address this research gap by refining the inlet wingwall and headwall configurations for square box and circular culverts. The first objective was to test rounded and tapered inlets as baselines, and compare the results with new wingwall and headwall angle combinations. The second objective was to evaluate the impact of aeration on culvert capacity under inlet control conditions.

Guidelines provide equations to calculate the head-to-discharge relationship but do not specify the percentage improvement that can be achieved with each specific inlet modification. Therefore, the third objective of this study was to quantify capacity improvements for different inlet configurations by developing a flow improvement coefficient, C_{TG}. This novel coefficient can be applied with the existing capacity equations for a standard square edge inlet culvert to determine the increased capacity. The magnitude of the coefficient would show the percentage capacity improvement obtained when using the specific inlet. The fourth objective was to verify that the experimental data for the standard square edge inlet under inlet control conditions align with the expected values from other guidelines and studies to justify the use of C_{TG} globally.

To address the study objectives, a series of physical model tests was conducted in a hydraulic flume to evaluate culvert performance under different inlet configurations.

EXPERIMENTAL SETUP

Physical models

The physical models consisted of various inlet configurations for square box and circular culverts. For this study:

- 30°, 45°, and 90° wingwalls as well as 15°, 30°, 45° and 90° headwalls were combined and tested. The 90° wingwall and 90° headwall represent the standard square edge inlet. Tapered inlets for box culverts are the same as wingwalls and headwalls for box culverts without an offset to the inlet.
- The circular culvert was tested with a 15° top taper and a 30° side taper.
- Both box and circular culverts were tested with a 0.25D rounded edge inlet.
- All configurations were tested with and without air vents.

Each model culvert tested, with its inlet modification, was positioned in the hydraulic flume, as shown in Figure 1. The flume is 450 mm wide, 500 mm high and 10 m long. A depth gauge (Depth Gauge 1) was placed 4D upstream of the model culvert; a measurement ruler was placed 0.75D upstream of the culvert inlet, which measured the headwater, H_1, and another depth gauge (Depth Gauge 2) was positioned 4D downstream of the culvert outlet.

The hydraulic flume has an adjustable slope. The slope was set to 1%, as recommended by the South African National Roads Agency Limited, as the minimum slope to prevent silt deposition (SANRAL 2013). The steep slope also ensured inlet control conditions for all the tests performed. Under inlet control conditions, the inlet geometry has a greater influence on the flow through the barrel than under outlet control (West 1956; Jones *et al.* 2006). The culvert with 30° wingwall and 15° headwall, as well as the 90° wingwall with a 90° headwall box culvert, was tested at slopes of 0%, 0.5%, 1.0%, and 1.5% to confirm the assertion by West (1956) that the effect of slope is almost completely negligible under submerged, inlet control conditions.

Inlet control also excludes the effects of roughness (Schall *et al.* 2012). Therefore, the models could be constructed from acrylic plastic and polylactic acid (PLA) filament, which are smoother than an actual culvert.

Froude uniformity for Free Surface Models (FSF) was used to scale the flow and velocity in the channel with no culvert model initially installed. The Reynolds number for the model channel was greater than 86,000. A Reynolds number of this magnitude in Froude uniformity ensures turbulent flow, where flow resistance remains nearly constant despite further increases in Reynolds number. The model culverts were made as large as possible to minimise the effect of surface tension. Model dimensions were limited by the size of the hydraulic flume, resulting in the following model culvert barrel sizes:

- Square box culvert: 200 mm × 200 mm.
- Circular culvert: internal diameter of 192 mm (the available acrylic plastic barrel size closest to 200 mm).

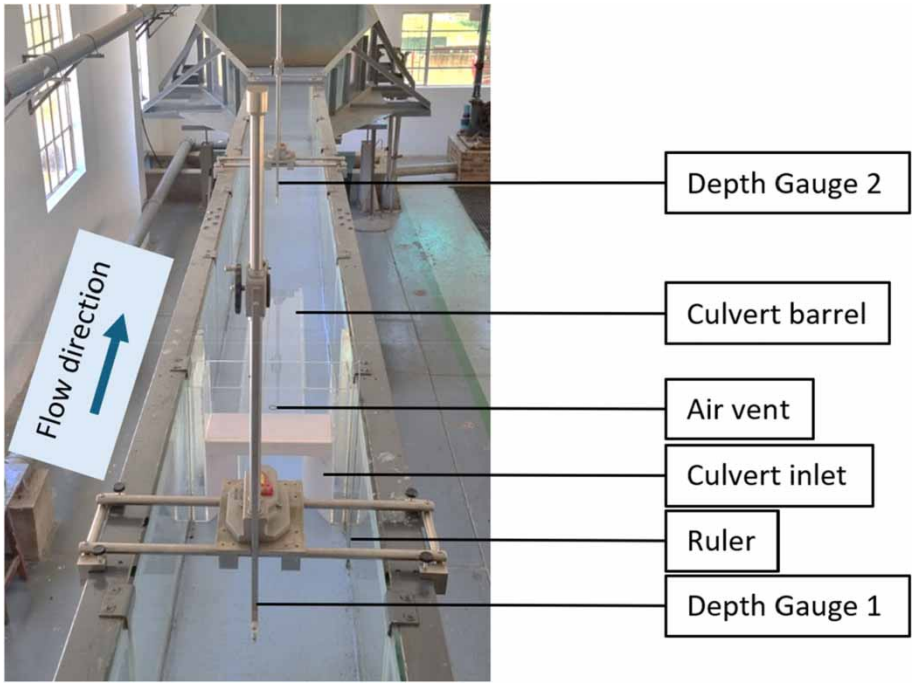

Figure 1 | Physical model setup in the hydraulic flume.

The prototype dimensions were obtained from a leading manufacturer of precast concrete products in South Africa (ROCLA 2017):

- Square box culvert: 600 mm × 600 mm.
- Circular culvert: 600 mm nominal diameter and 611 mm internal diameter.

The undistorted square box and circular culvert models were scaled based on these dimensions. This resulted in the box culverts having a scaling factor of 3, and the circular culverts a scaling factor of 3.18. The scaling dimensions for the box culverts are shown in Figure 2(a) and for the circular culverts in Figure 2(b). For all the models, the wingwalls extended 0.4D to the sides of the barrel, and the headwall extended 0.4D upward to ensure the enlarged inlet cross-sectional area of 360 mm × 280 mm was kept the same for all the tests, providing a consistent inflow area.

Each model culvert consisted of an acrylic plastic barrel with a 5-mm-diameter air vent, 0.85D from the inlet, which could be closed or opened. This distance was chosen to test the concept reported in a previous study (de Jager & van Dijk 2024). The model also had a 450 mm × 450 mm × 166 mm acrylic plastic inlet box designed to fit a 360 mm × 280 mm × 166 mm 3D-printed inlet. The 3D-printed inlet modification was replaced for each test. Silicone was used to seal the 3D-printed inlet within the acrylic plastic box and the acrylic plastic box in the hydraulic flume. Photos of the inlet models can be found in this experimental photos link (https://drive.google.com/drive/folders/1BmOVMU6H0GywmEmYi1E3tTQ1-kYoOKmHZ). These culvert models formed only one part of the overall experimental setup.

Testing procedure

The experimental setup is shown in Figure 3.

Water was pumped from the sump using submersible pumps (Pump 1 and Pump 2). The flow rate was controlled by adjusting any one of the three isolating valves (Valve 1, Valve 2 and Valve 3). The flow was measured using a FLOWmetrix SAFSONIC Fixed Ultrasonic Time of Flight Flowmeter. The data were logged with a HOBO 4-Channel Analog Data Logger and recorded every ten seconds. For the initial reading, all three isolating valves were kept fully open to achieve the lowest flow rate through the hydraulic flume, i.e. diverting flow back to the sump. Once the water stabilised, the water depth was measured upstream of the culvert (Depth Gauge 1), at the culvert inlet (Ruler) and downstream of the culvert (Depth Gauge 2). Potassium permanganate crystals were added at the culvert inlet to visualise the water flow behaviour. One of the valves was then partially closed to

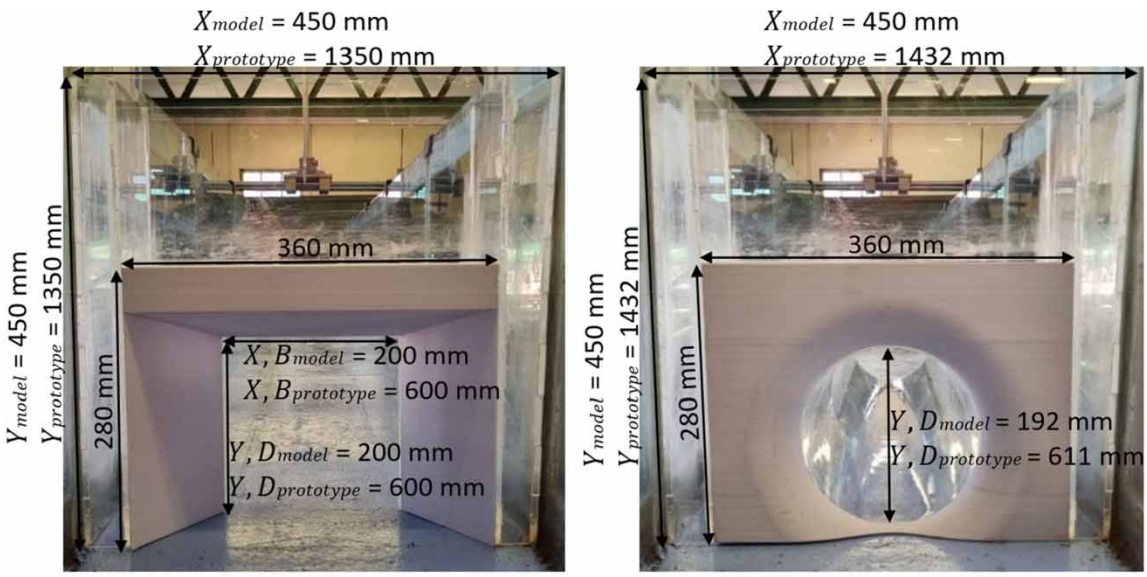

Figure 2 | Scaled dimensions for the (a) square box culverts and (b) circular culverts.

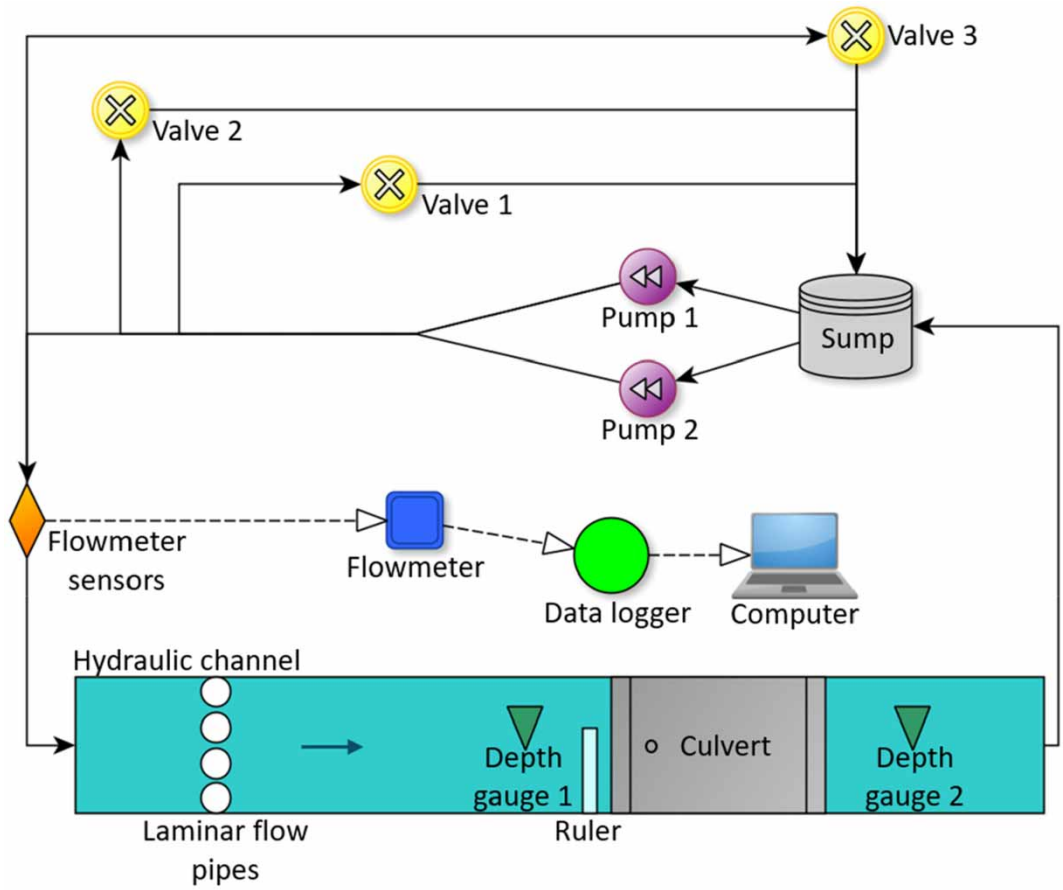

Figure 3 | Experimental setup.

increase flow through the hydraulic flume, after which the same measurement procedure was followed. For each test, the headwater depth and flow rate in the channel incrementally increased, with measurements taken until the headwater depth reached a maximum of 2*D*. The flow was then gradually decreased until the minimum flow rate was achieved again. Approximately 20 measurements were taken per test. For the same model, the air vent just after the inlet was opened, and the procedure was repeated to obtain another 20 measurements. The model was then removed, replaced with the next model, and properly sealed. Readings were also recorded manually to verify the logged flow data. Videos recorded during the experiments, showing the formation of air vortices at the culvert inlet and the flow behaviour for the different inlet types, highlighted by the addition of potassium permanganate crystals to the water, can be found in this experimental videos link (https://drive.google.com/drive/folders/1UDBTve_oddbOKN-DOFLa45R-6JEfQNdv).

The instrumentation precision and calibration are listed below:

- Water depth gauges that have an accuracy of ± 0.05 mm (Insize 2023) were calibrated with an Analog current-output pressure transducer, with a range of 0–1 bar and an output of 4–20 mA. The transducer has an accuracy of 0.25% FS (Gems Sensors 2022).
- The FLOWmetrix SAFSONIC Fixed Ultrasonic Time of Flight Flowmeter has an accuracy of ± 1% of the reading (FLOWmetrix 2016). It was calibrated using a SAFSONIC P Portable Ultrasonic Flowmeter.
- The HOBO 4-Channel Analog Data Logger has an accuracy of ± 0.001 mA or ± 0.2% of the reading (HOBO 2016). It was used to log both the flow from the flowmeter and the pressure from the pressure transducers simultaneously.

A third-degree polynomial trendline was fitted to the flow versus headwater data from the physical experiments to obtain a performance curve. This trendline was selected as it provided the best fit compared with polynomials of other degrees, as well as power and exponential functions. The residual analysis plot was used to determine if the regression model, a third-degree polynomial, fitted the data collected during the physical experiments and satisfied the key assumptions for accurate and reliable predictions (Qualtrics 2024). The residuals are randomly scattered around zero, smaller than 1.5 and larger than -1.5, with no clear pattern indicating that the model effectively captured the relationship between the independent and dependent variables. The actual flow obtained during the experiment was plotted against the model-predicted flow, showing a very strong linear relationship with an R^2 value near one. All R^2 values were higher than 0.9. The trendlines were, therefore, used to compare results with existing guidelines, evaluate flow improvements across inlet types, assess the effect of the air vent, and determine improvement coefficients for each modified configuration.

RESULTS

Comparison with previous guidelines/studies

The experimental data for the standard square edge inlet were compared with the expected values from the literature (Herr & Bossy 1972; Boyd 1987; Charbeneau 2005; *Hydraulic Design Manual* 2009; Schall *et al.* 2012; SANRAL 2013; Austroads 2023), under inlet control conditions. This was done to confirm consistency of these results with previously observed trends. The comparisons are shown in Figure 4(a) for box culverts and Figure 4(b) for circular culverts. As most existing culverts do not have air vents, experimental results for tests without air vents were compared with published trends. Since the results align with previous studies and guidelines, they can be used to compare different culvert inlet configurations.

Culvert inlet analysis

Figure 5 shows all the tests conducted for the different inlets, with a third-degree polynomial trendline fitted to each (a) square box culvert and (b) circular culvert inlet. Figure 5 displays the 1.2*D* threshold line since this is traditionally where flow changes from weir type to orifice type flow, and 2*D* is a criterion set by SANRAL (2013) for the maximum allowable headwater corresponding to a specific design recurrence interval.

In addition to the culvert inlet analysis, air vents were added to the inlet configurations to assess their effect on flow capacity.

Effect of air vents

Figure 6 shows a 30° wingwall and 15° headwall square box culvert as an example for a test with and without an air vent. All other box and circular culvert tests had similar results considering the air vent. The trendlines for the culvert with and without air vents are nearly identical, indicating the small influence of an air vent under inlet control conditions.

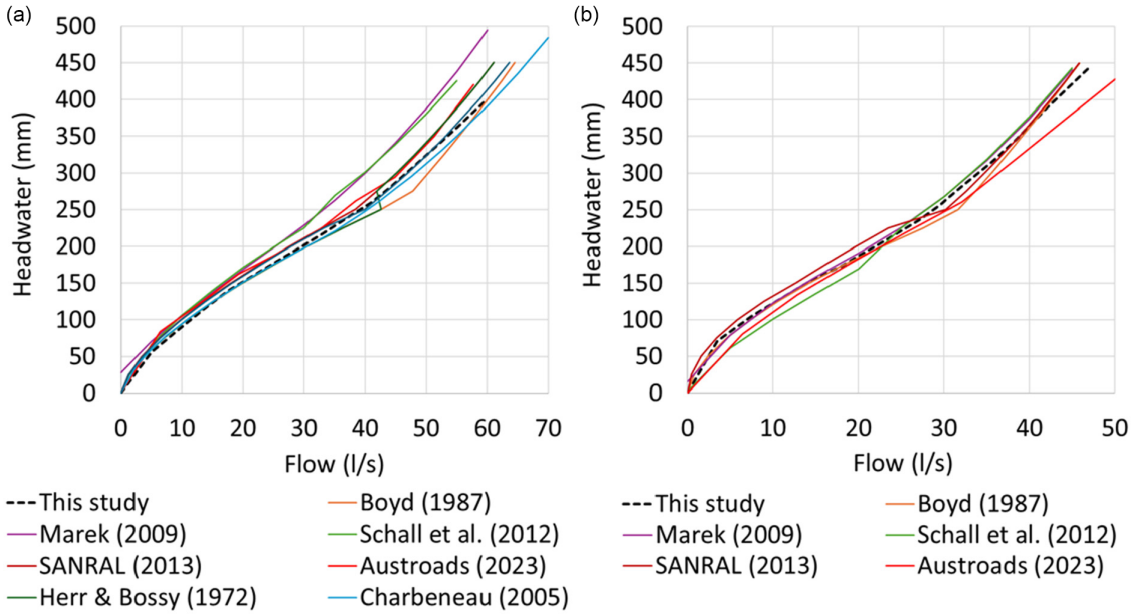

Figure 4 | Standard square edge inlet (a) box culvert and (b) circular culvert equations from the literature compared with the 90° wingwall and 90° headwall results.

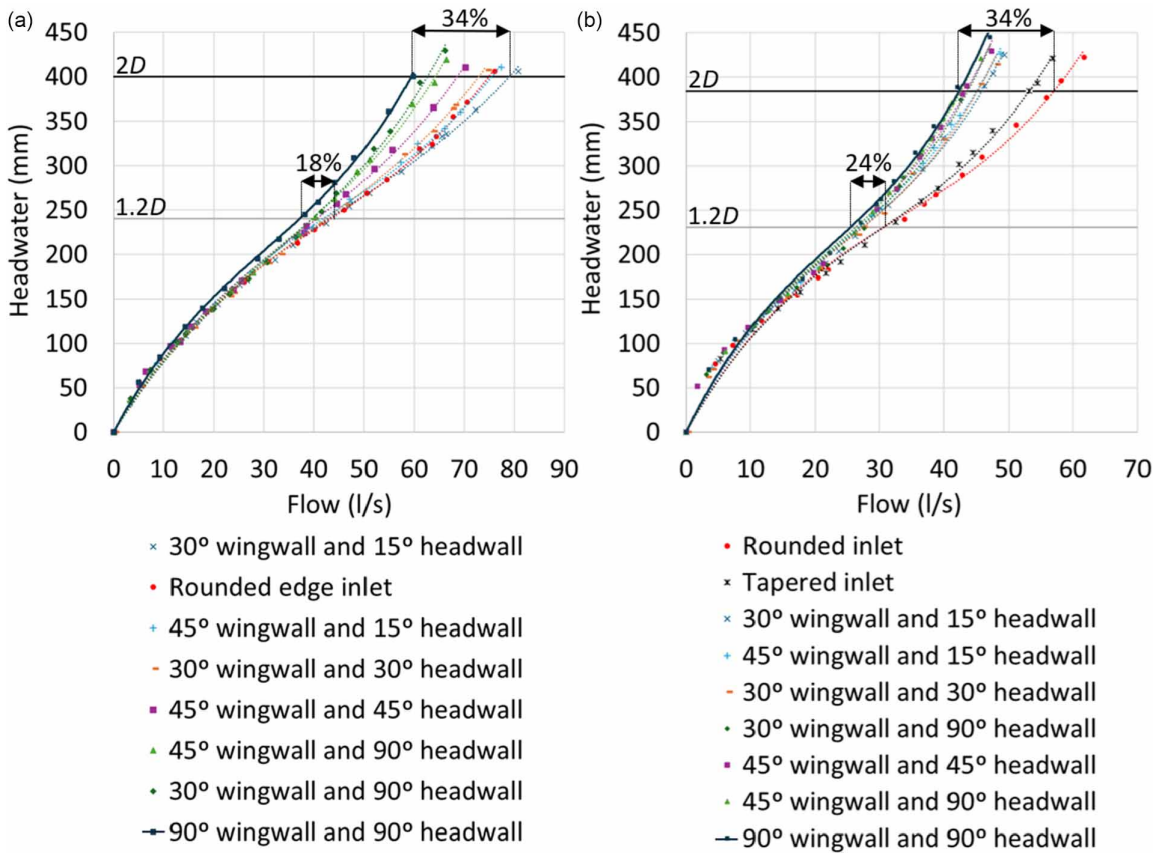

Figure 5 | Headwater-to-discharge relationship for improved (a) square box and (b) circular culvert inlets tested, ranked from most to least effective.

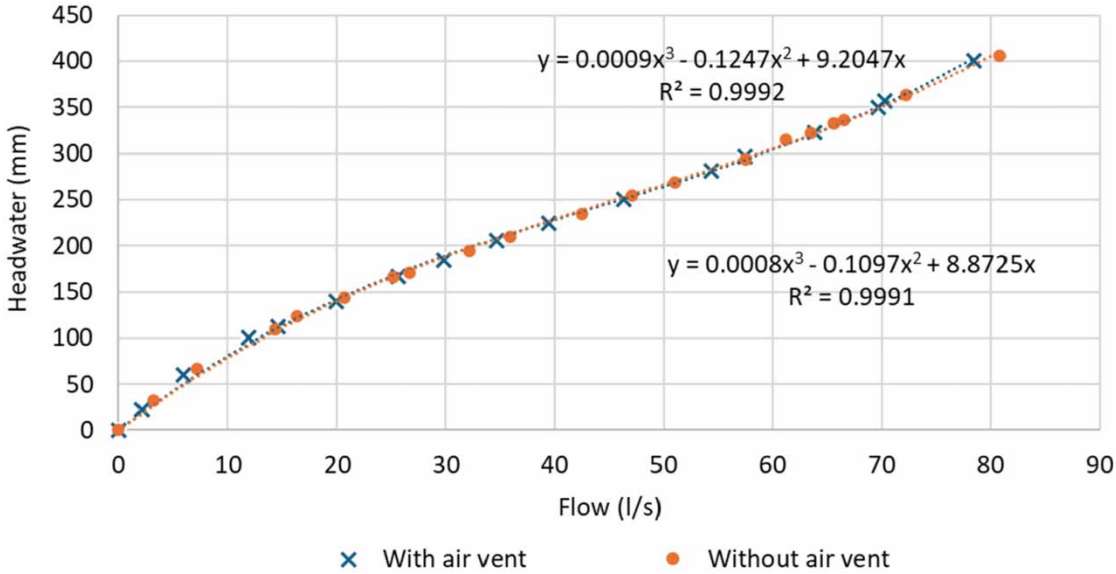

Figure 6 | Effect of the air vent on measured values for a 30° wingwall and 15° headwall square box culvert.

DISCUSSION

Comparison with previous guidelines/studies

The performance curves obtained from the experimental data for both square box and circular culverts are consistent with the performance curves from guidelines or other studies, as seen in Figure 4(a) for box culverts and Figure 4(b) for circular culverts. It should, therefore, be possible to compare results from different inlet configurations and apply the improvement coefficients developed in this study to adjust values estimated using any relevant equations from the literature.

Culvert inlet analysis

Figure 5(a) shows that for headwater elevations up to 1D, all squared box culvert inlet improvement resulted in small increases in flow, typically less than 15%. The inlet improvement had a considerable influence when the inlet was submerged. The 30° wingwall with a 15° headwall provided the greatest improvement in hydraulic performance due to smoother flow alignment, reduced inlet turbulence, improving contraction and discharge efficiency. The 30° wingwall with a 15° headwall increased flow by 34% at $H_1/D = 2$. It was followed by a rounded edge inlet and a 45° wingwall with a 15° headwall. The impact of an angled headwall is evident, especially with a 15° headwall, as the smaller angle causes less contraction after the inlet. However, the smallest angle of 0° performed the worst, as it effectively reverts to a square edge inlet. A 30° wingwall with a 15° headwall increased flow 29% more compared with a 30° wingwall with a 90° headwall. The maximum discharge capacity for a 200 mm × 200 mm model square box culvert with an inlet improvement was 79.9 l/s at $H_1/D = 2$, compared with 59.5 l/s without the inlet improvement, representing an improvement of 20.4 l/s through the model culvert. The experimental flow rate of 79.9 l/s corresponds to an actual flow of 1,246 l/s for a 600 mm × 600 mm box culvert, resulting in an actual flow improvement of 319 l/s.

Circular culverts always have an offset between the circular inlet and the wingwalls or headwalls, causing water to break away at the circular inlet face and decreasing the discharge capacity. Figure 5(b) shows that both wingwalls and headwalls provided a limited increase in flow, while the tapered and rounded edge inlets significantly increased flow, especially once the inlet was submerged. This indicates the importance of guiding water to flow smoothly into the precise barrel shape. The barrel of the rounded edge inlet flowed almost completely full at $H_1/D = 2$, resulting in a 34% flow increase. The 30° wingwall with a 15° headwall performed the best across all wingwalls and headwalls but increased flow only by 9% at $H_1/D = 2$. The maximum flow that a 192 mm diameter circular culvert model could convey at $H_1/D = 2$ was 57.3 l/s with the best inlet improvement and 42.8 l/s without an inlet improvement, representing a flow improvement of 14.5 l/s through the model culvert. The experimental flow rate of 57.3 l/s corresponds to an actual flow of 1,035 l/s for a circular culvert with a

nominal diameter of 600 mm, resulting in an actual flow improvement of 262 l/s. These same inlet configurations were also analysed with air vents near the culvert inlet.

Effect of air vents

The trendlines, shown in Figure 6 for the culvert with and without air vents are nearly identical, indicating the small influence of an air vent under inlet control conditions. The percentage difference in flow between a culvert with and without an air vent was calculated using Equation (1):

$$\text{Percentage flow difference (\%)} = \frac{(Q_{\text{with airvent}} - Q_{\text{without airvent}})}{Q_{\text{without airvent}}} \times 100 \quad (1)$$

The air vent changed the flow across all inlet modifications for the square box culvert by a maximum of 2.7%. Flow through the circular culvert inlets was changed by a maximum of 2.0% except for the rounded edge inlet. For the rounded edge inlet, circular culvert flow improved with a maximum of 3.3% at $H_1/D = 1.67$, but overall, between headwater elevations of $1.3D$ and $2D$, which was when the culvert barrel flowed almost completely full. This suggests that the use of an air vent could enhance the discharge through the culvert under inlet control, supporting the concept of a barrel flowing almost completely full to enhance the flow through a conduit (Chadwick *et al.* 2021). Further investigation is recommended as the measured improvement was minor. As a result, the flow improvement coefficient was determined using culverts without air vents.

Flow improvement coefficients

The results from this study were used to develop a coefficient for flow improvement, C_{TG}. This coefficient can be used to determine the improved culvert discharge caused by each inlet modification. It can be applied as an adjustment factor to the discharge for a standard square edge inlet culvert calculated using existing guidelines/formulae, as shown in Equation (2). Equation (2) also indicates that the greater the C_{TG} coefficient, the better the culvert performance:

$$Q_{\text{Improved}} = Q_{\text{Square edge inlet culvert}} \times C_{TG} \quad (2)$$

Equation (3) was used to calculate the percentage flow increase to quantify the flow improvement for each inlet compared with the standard square edge inlet:

$$\text{Flow improvement (\%)} = \frac{(Q_{\text{Improved inlet}} - Q_{\text{Square edge inlet}})}{Q_{\text{Square edge inlet}}} \times 100 \quad (3)$$

For any specific headwater level larger than $H_1/D = 0.5$, the coefficient can be calculated with Equation (4) using the flow improvement percentage calculated with Equation (3).

$$C_{TG} = \frac{\text{Flow improvement (\%)}}{100} + 1 = \frac{(Q_{\text{Improved inlet}} - Q_{\text{Square edge inlet}})}{Q_{\text{Square edge inlet}}} + 1 \quad (4)$$

Figure 7 shows the improvement coefficients for a 30° wingwall and 15° headwall square box culvert as a typical example. The amount of flow improvement for a specific inlet modification changes as the flow or headwater level changes. Therefore, the C_{TG} coefficients can be linked to an H_1/D value or a range of H_1/D values. The coefficients were plotted separately for unsubmerged inlet headwater elevations, $0.5 \leq H_1/D \leq 1.2$, and submerged inlet headwater elevations, $1.2 < H_1/D \leq 2$. A trendline was fitted through each section to obtain an equation that can be used to calculate the C_{TG} coefficient depending on the H_1/D ratio.

Since wingwalls and headwalls had a significant impact on the discharge capacity of square box culverts, the C_{TG} coefficients for different wingwall- and headwall-angle box culverts at a headwater depth of $1.2D$ are shown in Figure 8(a) and at a headwater depth of $2D$ are shown in Figure 8(b). The C_{TG} coefficients show their percentage improvement; for example, an inlet with a C_{TG} coefficient of 1.34 provides a 34% increase at that specific headwater depth. A contour chart was generated by interpolating between the coefficients calculated from the results. The contour chart allows for determining coefficients for different wingwall and headwall angles and gives a visual indication towards the optimal angles. Figure 8(a)

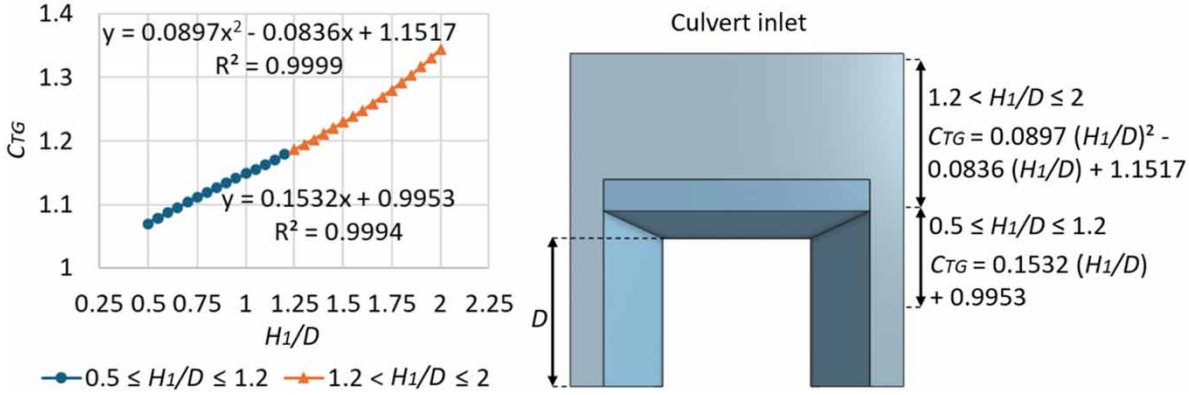

Figure 7 | C_{TG} coefficient equations for a 30° wingwall and 15° headwall square box culvert.

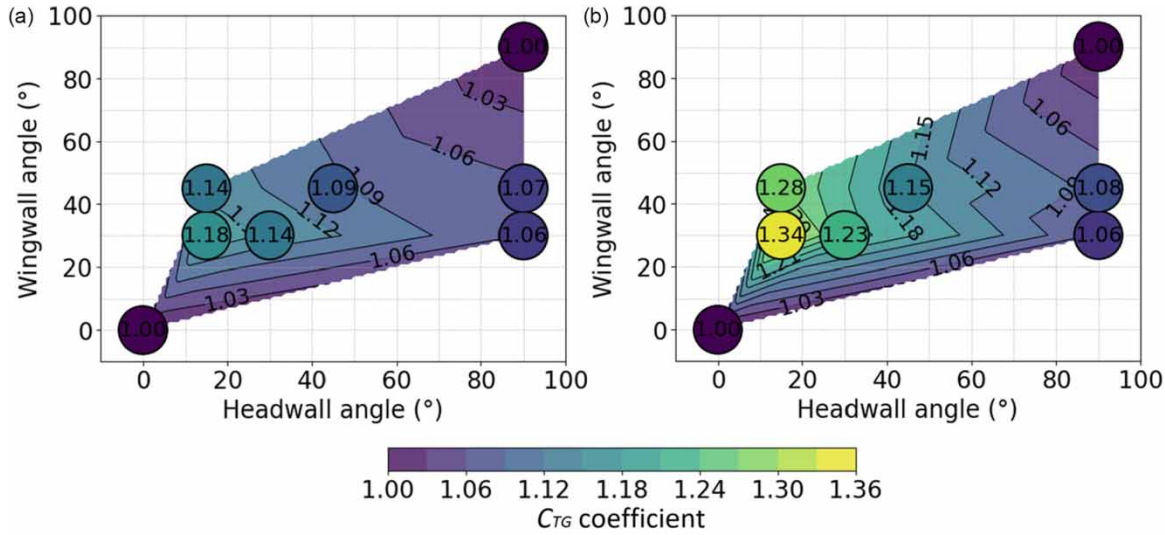

Figure 8 | C_{TG} coefficients for the different wingwall and headwall angles at a headwater of (a) 1.2D and (b) 2D.

and 8(b) indicate that the optimal wingwall angle lies between 0° and 30°, and the optimal headwall angle falls between 0° and 15°. All the other areas will, therefore, also be populated with measured values to determine the optimal wingwall and headwall angles. However, for the most-used wingwall angles and the best-performing headwalls from the literature that were tested in this study, the 30° wingwall and 15° headwall provide the greatest increase in discharge. For wingwalls larger than 30° and headwalls larger than 15°, Figure 8(a) shows that at $H_1 = 1.2D$, the wingwall and headwall angles almost evenly contribute to the increase in culvert performance. From Figure 8(b), it is clear that the angle of the headwall has a much larger influence than a wingwall at $H_1 = 2D$. The headwall, therefore, has a much larger influence at high flows when the inlet is submerged.

For box culverts especially, it would be feasible to optimise headwalls and wingwalls that are already commonly used as retaining structures. The inlet improvements for box culverts in this study were based on a square culvert, which did not account for the exact contribution of a wingwall and a headwall for different sizes of rectangular culverts and should be considered in further research. From Figure 8, the 30° wingwall and 15° headwall provide the best culvert performance from all the tested combinations. A combination of different wingwall and headwall angles might be the solution to optimise the angles. However, the same, smaller angle, such as a 15° wingwall with a 15° headwall, should also be tested to confirm the effectiveness. The C_{TG} coefficient equations for a 30° wingwall and 15° headwall square box culvert were compared with the C_{TG} coefficient equations of a rounded edge inlet in Table 2. Table 2 also provides the percentage flow improvement for each inlet modification at a headwater depth of 1.2D and 2D, as well as the standard square edge inlet equations from

Table 2 | Inlet-controlled square box culvert improvement coefficient equations and their percentage improvement in discharge capacity

SANRAL (2013)	C_{TG} coefficient equations
For: $0 < H_1/D \leq 1.2$	Equations only apply for $0.5 \leq H_1/D \leq 1.2$
$Q = \frac{2}{3} C_B B H_1 \sqrt{\frac{2}{3} g H_1}$	**30° wingwall and 15° headwall (18% at 1.2*D*)**
Where: $C_B = 0.9$	$C_{TG} = 0.1532(H_1/D) + 0.9953$
	Rounded edge inlet (17% at 1.2*D*)
	$C_{TG} = 0.1851(H_1/D) + 0.9572$
For: $H_1/D > 1.2$	Equations only apply for $1.2 < H_1/D \leq 2$
$Q = C_h B D \sqrt{2g(H_1 - C_h D)}$	**30° wingwall and 15° headwall (34% at 2*D*)**
	$C_{TG} = 0.0897(H_1/D)^2 - 0.0836(H_1/D) + 1.1517$
Where: $C_h = 0.6$	**Rounded edge inlet (26% at 2*D*)**
	$C_{TG} = -0.0011(H_1/D)^2 + 0.1150(H_1/D) + 1.0363$

Table 3 | Inlet-controlled circular culvert improvement coefficient equations and their percentage improvement in discharge capacity

SANRAL (2013)	C_{TG} coefficient equations
For: $0 < H_1/D \leq 0.8$	Equations only apply for $0.5 \leq H_1/D \leq 1.2$
$\frac{Q}{D^2\sqrt{gD}} = 0.48\left(\frac{S_0}{0.4}\right)^{0.05}\left(\frac{H_1}{D}\right)^{1.9}$	**30° wingwall and 15° headwall (8% at 1.2*D*)**
For: $0.8 < H_1/D \leq 1.2$	$C_{TG} = 0.0710(H_1/D) + 0.9950$
$\frac{Q}{D^2\sqrt{gD}} = 0.44\left(\frac{S_0}{0.4}\right)^{0.05}\left(\frac{H_1}{D}\right)^{1.5}$	**Rounded edge inlet (24% at 1.2*D*)**
	$C_{TG} = 0.3473(H_1/D) + 0.8386$
	Tapered inlet (21% at 1.2*D*)
	$C_{TG} = 0.2314(H_1/D) + 0.9484$
For: $H_1/D > 1.2$, the orifice formula applies.	Equations only apply for $1.2 < H_1/D \leq 2$
$Q = C_D A \sqrt{2g\left(H_1 - \frac{D}{2}\right)}$	**30° wingwall and 15° headwall (9% at 2*D*)**
Where: $C_D \approx 0.6$	$C_{TG} = -0.0262(H_1/D)^2 + 0.0949(H_1/D) + 0.9998$
	Rounded edge inlet (34% at 2*D*)
	$C_{TG} = -0.0734(H_1/D)^2 + 0.3598(H_1/D) + 0.9127$
	Tapered inlet (25% at 2*D*)
	$C_{TG} = -0.0739(H_1/D)^2 + 0.2874(H_1/D) + 0.9747$

SANRAL (2013) as an example of existing guidelines to which the coefficients can be applied. The C_{TG} coefficient equations for a 30° wingwall and 15° headwall circular culvert are compared with the C_{TG} coefficient equations of a rounded edge and tapered inlet in Table 3.

The C_{TG} coefficient is also shown to be valid across different culvert sizes. Figure 9 presents a comparison between a 200 mm × 200 mm and a 600 mm × 600 mm box culvert. In both Figure 9(a) and 9(b), the coefficient was applied to the standard square edge inlet SANRAL (2013) design equations to determine the improved flow resulting from the addition of a 30° wingwall and 15° headwall. Experimental headwater depth and flow data for both the square edge inlet and the improved inlet configuration on the 200 mm × 200 mm culvert were plotted and scaled to a 600 mm × 600 mm culvert using Froude uniformity.

The 30° wingwall with a 15° headwall and the 90° wingwall with a 90° headwall were also tested at slopes of 0%, 0.5%, 1.0%, and 1.5%, with no substantial performance differences, supporting West's (1956) finding that slope has a negligible effect for submerged inlet-controlled flow. Multi-barrel culverts were also not tested, as Jones *et al.* (2006) concluded that inlet improvement coefficients from single-barrel culverts are applicable.

C_{TG} coefficients are therefore assumed valid across these slopes and for multi-barrel culverts. However, further testing is recommended to confirm whether this will be applicable for additional slopes, multi-barrel culverts, culvert roughness, added embankments and other practical considerations discussed in the next section.

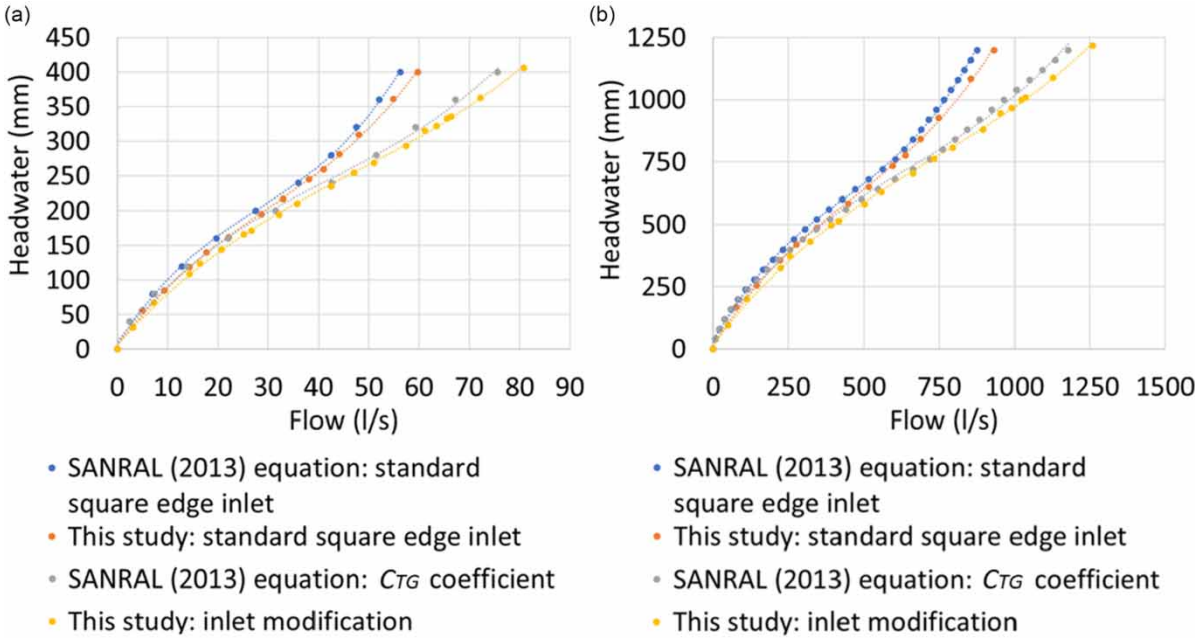

Figure 9 | Applicability of C_{TG} coefficient for different culvert sizes: (a) 200 mm × 200 mm box culvert and (b) 600 mm × 600 mm box culvert.

Practical implementation considerations

While this study's inlet modifications have shown benefits under ideal conditions, the flume size (450 mm × 500 mm) limited the model scale and flow depth to 2*D*. Water levels fluctuated slightly (±2 mm, up to ±10 mm at higher flows), and flow rates from the flowmeter varied by ±4 l/s. Although average values over time were taken for each reading, trendlines helped reduce variability and showed good agreement with previous studies and guidelines. Minor irregularities, such as silicone sealing and model assembly, may have slightly influenced the results. As this is a small-scale study, full-scale validation is recommended.

CFD models can also be used to assess performance under non-ideal conditions such as misalignment, debris, and silt at the inlet, all of which can significantly influence culvert performance. Jaeger (2019) recommended rounded and tangential inlet modifications for misaligned culverts, as misalignment increases head losses, reduces discharge capacity, and increases the risk of sedimentation and erosion. To mitigate debris accumulation, structural measures such as debris deflectors or screens can intercept and redirect debris or guide it more effectively through the culvert (Schall *et al.* 2012). Inlet improvements are expected to assist in aligning flow and guiding debris through the culvert, though further investigation is necessary to confirm this.

Flow improvement was most noticeable under submerged conditions, which is advantageous during high flood events. Testing at headwater levels above 2*D* is recommended, but such depths should not be used for design due to embankment instability and piping risks.

Culvert upgrades typically require pipe jacking or trench excavation, the latter often being less costly but more disruptive due to traffic delays and extended construction time. Inlet modifications offer a more cost-effective alternative (Straub *et al.* 1953; Jaeger 2019); however, further evaluation is needed to quantify the exact cost benefits across different inlet types and scenarios.

CONCLUSIONS

The culvert inlet directly affects the flow through the culvert, as seen in Figure 10. For a square edge inlet, sharp flow contraction leads to a higher headwater level (H_1), with a low water depth and high velocity within the barrel. An improved inlet reduces flow separation, producing a lower H_1, and fuller barrel flow with lower velocities. Although discharge remains the same in both cases, the improved inlet reduces upstream water levels and potential flood impacts.

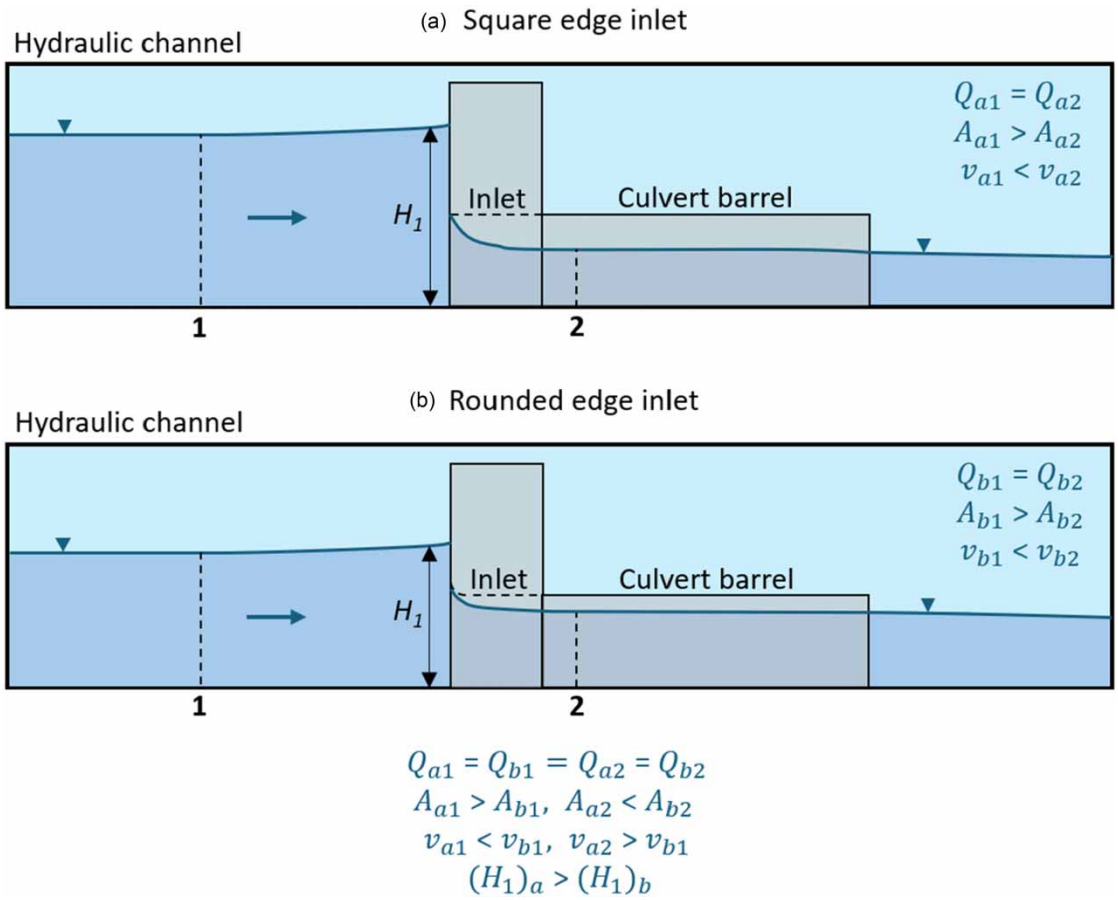

Figure 10 | Comparison of side views of the same flow rate in a culvert with (a) a square edge inlet and (b) a rounded edge inlet.

Using physical modelling, this study showed that modifying a culvert inlet for both square box and circular culverts can improve culvert discharge by up to 34%, considering a specific headwater depth. This is a significant increase in flow for a small, cost-effective retrofit compared with rebuilding an entire existing structure or when designing a new culvert structure for exceedance. For this study:

- A combination of wingwall and headwall angles, such as the 30° wingwall and 15° headwall, performed the best. This might be the solution to optimise the angles. Headwalls have a greater influence on the discharge capacity than the wingwalls when the headwater level reaches 2*D*.
- Optimised headwalls and wingwalls increased the discharge capacity more than with rounded inlet edges for the square box culvert. For circular culverts, it would be more beneficial to round the inlet edges, guiding water directly to the circular inlet circumference or to the perimeter, as in the case of other inlet shapes.
- Capacity improvements for the different inlets tested were quantified by developing a flow improvement coefficient, C_{TG}, for inlet control conditions. For a specific headwater depth, the C_{TG} coefficient value gives the percentage flow improvement with the decimal places; for example, an inlet with a C_{TG} coefficient of 1.34 provides a 34% increase in discharge capacity.
- The experimental data align with existing culvert capacity equations for a standard square edge inlet. Therefore, the coefficient can be applied to the different existing guidelines/formulae to determine the increased capacity. This can help design or upgrade culverts.
- The air vent did not have a significant influence on the culvert capacity under inlet control conditions. An air vent installed at different locations and tested under both inlet and outlet control is necessary to gain a clearer understanding of the magnitude of its influence.

The best inlet modification may increase the hydraulic capacity the most; however, site conditions and existing characteristics may dictate the improvement. For example, a site with existing 45° wingwalls may not perform as well as with 30° wingwalls; however, rather than deconstructing and rebuilding, only a sloped headwall could be added, providing the required additional capacity.

RECOMMENDATIONS

It is recommended that this research be expanded through a combination of physical modelling, computational fluid dynamics (CFD) simulations, and full-scale case studies to test:

- alternative culvert inlet modifications under both inlet and outlet control and to determine their corresponding C_{TG} coefficient equations;
- additional wingwall and headwall combinations to expand the C_{TG} coefficient contour chart in Figure 8, and identify optimal configurations.

While the C_{TG} coefficient aligns with existing guidelines such as SANRAL (2013), Austroads (2023) and Schall *et al.* (2012), as seen in Figure 4, further testing and sensitivity analyses are needed to confirm its broader applicability across various culvert types and global contexts.

ACKNOWLEDGEMENTS

Special thanks to Mr Jan Ngwenya for assisting with laboratory testing, to Mr Jordan Mostert for installing instrumentation and managing the 3D printing and to Kekeletso Ramanamane for additional testing.

FUNDING

This study was supported by the South African National Roads Agency SOC Limited (SANRAL) (Project number: 1002-58600-2018-P7a.10) and the Water Research Commission (WRC) (Project number: C2023/2024-01295).

ETHICS: HUMAN PARTICIPANTS

This study did not involve human participants, and therefore no ethics approval was required.

ETHICS: ANIMAL TESTING

This study did not involve animal testing, and therefore no ethical approval was required.

DATA AVAILABILITY STATEMENT

All relevant data are included in the paper or its Supplementary Information. Photos of the inlet models can be found at https://drive.google.com/drive/folders/1BmOVMU6H0GywmEmYi1E3tTQ1kYoOKmHZ. Videos recorded during the experiments, showing the formation of air vortices at the culvert inlet and the flow behaviour for the different inlet types, can be found at https://drive.google.com/drive/folders/1UDBTve_oddbOKN-DOFLa45R-6JEfQNdv.

CONFLICT OF INTEREST

The authors declare there is no conflict.

REFERENCES

Abreu, V. H. S. d., Santos, A. S. & Monteiro, T. G. M. (2022) Climate change impacts on the road transport infrastructure: a systematic review on adaptation measures, *Sustainability*, **14** (14), 8864. https://doi.org/10.3390/su14148864.

Aly, T. E. (2017) Improving the pipe culvert efficiency by using inclined headwalls, *International Water Technology Journal, IWTJ*, **7** (1), 26–36.

Ashour, M. A., Aly, T. E. & Abdou, A. A. (2016) Inclined headwall is an efficient tool for maximizing the discharge efficiency through culverts'. In: Gâştescu, P. & Bretcan, P. (eds) *3rd International Conference: Water Resources and Wetlands*. Târgoviște, Romania: Romanian Limnogeographical Association, pp. 184–193

Austroads (2023) *Guide to Road Design Part 5B: Drainage – Open Channels, Culverts and Floodway Crossings*. AGRD05B-23, Sydney, NSW, Australia: Austroads Ltd.

Boyd, M. J. (1987) Generalised head-discharge equations for culverts. In: *Fourth National Local Government Engineering Conference 1987*. Barton, ACT, Australia: Institution of Engineers, pp. 161–165.

Buck, G. & Allitt, R. (2019) The importance of culvert inlets. In: *Chartered Institution of Water and Environmental Management Urban Drainage Group Spring Conference 2019*, paper 4.

Chadwick, A., Morfett, J. & Borthwick, M. (2021) *Hydraulics in Civil and Environmental Engineering*, 6th edn. Abingdon, UK and Boca Raton, FL, USA: CRC Press.

Charbeneau, R. J. (2005) *Hydraulics of Low-Headwater Box Culverts*. University of Texas at Austin, Austin, TX, USA: Center for Transportation Research.

Cullis, J., Alton, T., Arndt, C., Cartwright, A., Chang, A., Gabriel, S., Gebretsadik, Y., Hartley, F., de Jager, G., Makrelov, K., Robertson, G., Schlosser, C. A., Strzepek, K. & Thurlow, J. (2015) *An Uncertainty Approach to Modelling Climate Change Risk in South Africa*. WIDER Working Paper 2015/045, Helsinki, Finland: United Nations University World Institute for Development Economics Research.

de Jager, L. & van Dijk, M. (2024) Improvements to the hydraulic performance of culverts under inlet control conditions by optimisation of inlet characteristics, *Water*, **16** (11), 1569. https://doi.org/10.3390/w16111569.

FLOWmetrix (2016) *User's Guide Installation & Operation Instructions: SAFSONIC F Fixed Ultrasonic Time of Flight Meter*. Durban, South Africa: FLOWmetrix. Available at: http://www.flowmetrix.co.za/.

French, J. L. (1955) *First Progress Report on Hydraulics of Short Pipes: Hydraulic Characteristics of Commonly Used Pipe Entrances*. NBS Report 4444, Washington, DC, USA: US National Bureau of Standards.

French, J. L. (1961) *Fourth Progress Report on Hydraulics of Culverts: Hydraulics of Improved Inlet Structures for Pipe Culverts*. NBS Report 7178, Washington, DC, USA: US National Bureau of Standards.

French, J. L. (1964) Tapered inlets for pipe culverts, *Journal of the Hydraulics Division*, **90**, 255–299.

Gems Sensors (2022) Gems Sensors Pressure Sensor, 1bar Max, Analogue Output, Relative Reading. Available at: https://in.rsdelivers.com/product/gems-sensors/3500b0001g01b000/gems-sensors-pressure-sensor-1bar-max-analogue/8968421?srsltid=AfmBOoqXfbChFtdsAYDXSuRi4rKEwIs-ii4DRpLOfhkZuFaym0UE4I_3 (accessed: 16 October 2024).

Harrison, L. J., Morris, J. L., Normann, J. M. & Johnson, F. L. (1972) *Hydraulic Design of Improved Inlets for Culverts*. Hydraulic Engineering Circular No. 13, FHWA/EO-72-13, Washington, DC, USA: Federal Highway Administration, US Department of Transportation.

Herr, L. A. & Bossy, H. G. (1972) *Capacity Charts for the Hydraulic Design of Highway Culverts*. Hydraulic Engineering Circular No. 10, Washington, DC, USA: Federal Highway Administration, US Department of Transportation.

HOBO (2016) *HOBO 4-Channel Analog Data Logger (UX120-006M) Manual*. Bourne, MA, USA: Onset Computer Corporation. Available at: https://www.onsetcomp.com/sites/default/files/resources-documents/17384-E%20UX120-006M%20Manual.pdf.

Hydraulic Design Manual (2009) *Hydraulic Design Manual*. Austin, TX, USA: Design Division, Texas Department of Transportation.

Insize (2023) Height Measuring Instruments, Dial Height Gage. Available at: https://insize.com/page-23-911.html (accessed: 2 November).

Jaeger, R. (2019) *Hydraulic Improvements in Culverts for Climate Change Adaptation*. PhD thesis. University of the Sunshine Coast.

Jaeger, R., Tondera, K., Pather, S., Porter, M., Jacobs, C. & Tindale, N. (2019) Flow control in culverts: a performance comparison between inlet and outlet control, *Water*, **11** (7), 1408. https://doi.org/10.3390/w11071408.

Jones, J. S., Kerenyi, K. & Stein, S. (2006) *Effects of Inlet Geometry on Hydraulic Performance of Box Culverts*. FHWA-HRT-06-138, McLean, VA, USA: Federal Highway Administration.

Kirshen, P., Caputo, L., Vogel, R. M., Mathisen, P., Rosner, A. & Renaud, T. (2014) Adapting urban infrastructure to climate change: a drainage case study, *Journal of Water Resources Planning and Management*, **141** (4), 04014064. https://doi.org/10.1061/(ASCE)WR.1943-5452.0000443.

Lallemant, D., Hamel, P., Balbi, M., Lim, T. N., Schmitt, R. & Win, S. (2021) Nature-based solutions for flood risk reduction: a probabilistic modeling framework, *One Earth*, **4** (9), 1310–1321. https://doi.org/10.1016/j.oneear.2021.08.010.

Pamungkas, A. & Purwitaningsih, S. (2019) Green and grey infrastructures approaches in flood reduction, *International Journal of Disaster Resilience in the Built Environment*, **10** (5), 343–362. https://doi.org/10.1108/IJDRBE-03-2019-0010.

Qualtrics (2024) Interpreting Residual Plots to Improve Your Regression. Available at: https://www.qualtrics.com/support/stats-iq/analyses/regression-guides/interpreting-residual-plots-improve-regression/ (accessed: 9 October 2024).

ROCLA (2017) *ROCLA Product Catalogue*. Roodeport, South Africa: ROCLA. Available at: http://www.rocla.co.za/wp-content/uploads/2018/08/rocla-product-catalogue.pdf.

SANRAL (2013) *Drainage Manual*, 6th edn. Pretoria, South Africa: The South African National Roads Agency SOC Ltd.

Schall, J. D., Thompson, P. L., Zerges, S. M., Kilgore, R. T. & Morris, J. L. (2012) *Hydraulic Design of Highway Culverts*, 3rd edn. Hydraulic Design Series No. 5, FHWA-HIF-12-026, Washington, DC, USA: Federal Highway Administration.

Schütte, S. & Schulze, R. E. (2017) Projected impacts of urbanisation on hydrological resource flows: a case study within the uMngeni catchment, South Africa, *Journal of Environmental Management*, **196**, 527–543. https://doi.org/10.1016/j.jenvman.2017.03.028.

Sellevold, J., Bruland, O. & Pummer, E. (2023) Hydraulic efficiency and optimization of pipe culvert inlet edges, *VANN*, **58** (4), 235–250.

Skidmore, P. & Wheaton, J. (2022) Riverscapes as natural infrastructure: meeting challenges of climate adaptation and ecosystem restoration, *Anthropocene*, **38**, 100334. https://doi.org/10.1016/j.ancene.2022.100334.

Straub, L. G., Anderson, A. G. & Bowers, C. E. (1953) *Importance of Inlet Design on Culvert Capacity*. Technical Paper No. 13, Series B, Minneapolis, MN, USA: St Anthony Falls Hydraulic Laboratory, University of Minnesota.

Wasko, C., Nathan, R., Stein, L. & O'Shea, D. (2021) Evidence of shorter more extreme rainfalls and increased flood variability under climate change, *Journal of Hydrology*, **603**, 126994. https://doi.org/10.1016/j.jhydrol.2021.126994.
West, E. M. (1956) *Hydraulic Model Studies of Culvert Operation*. Lexington, KY, USA: Highway Materials Research Laboratory.
Yarnell, D. L., Nagler, F. A. & Woodward, S. M. (1926) *Flow of Water through Culverts*. Iowa City, IA, USA: University of Iowa.

First received 7 February 2025; accepted in revised form 28 June 2025. Available online 15 July 2025